AAS 05-103

OPTIMAL CONFIGURATION OF SPACECRAFT FORMATIONS VIA A GAUSS PSEUDOSPECTRAL METHOD

Geoffrey T. Huntington* and Anil V. Rao†

The problem of determining minimum-fuel maneuver sequences for a four-spacecraft formation is considered. The objective of this paper is to determine fuel-optimal configuration trajectories that transfer a four spacecraft formation from an initial parking orbit to a desired terminal reference orbit while satisfying particular formation constraints. In this paper, the configuration problem is solved numerically using a newly developed direct transcription method called the *Gauss pseudospectral method*. Two versions of the minimum-fuel configuration problem are considered. In the first problem the trajectory is terminated upon satisfying the required terminal position constraints. In the second problem the trajectory is extended one full orbit beyond that of the first problem such that the terminal conditions are the same as those attained one period earlier. The results obtained in this paper illustrate the key features of the optimal configuration trajectories and controls, provide insight into the structure of the optimally controlled system, and demonstrate the applicability of the Gauss pseudospectral method to optimal formation flying trajectory design.

1 INTRODUCTION

Spacecraft formation flying is defined as a set of more than one spacecraft whose states are coupled through a common control law.[1] Formation flying has been identified as an enabling technology for many future space missions. In particular, space missions using multiple spacecraft, as compared with using a single spacecraft, allow simultaneous measurements to be taken at specific relative locations, thereby improving science return. An important aspect that is critical to the successful implementation of formation flying missions is trajectory design (also called *path planning* or *guidance*[2]). An excellent survey of methods used to design trajectories for formation flying can be found in Ref. 2. Also, Ref. 2 provides an extensive list of references on formation flying guidance. Formation flying trajectory design has two main categories: *stationkeeping*, i.e. to maintain a specified relative formation between a cluster of spacecraft for a specified portion of the trajectory and *reconfiguration*, i.e. to maneuver a cluster of spacecraft from one formation to a second formation.

In this paper we consider a specific optimal configuration problem sometimes referred to as an orbit insertion problem or an initialization problem.[3] The trajectory must optimally transfer four spacecraft from an initial circular parking orbit to an elliptic reference orbit of the same inclination while simultaneously satisfying a set of constraints on the relative location of the four spacecraft near the apogee of the terminal reference orbit. The relative position constraints of the four spacecraft are imposed by placing constraints on the volume and position relative to the mesocenter (or mean position) of a desired tetrahedron. While in principle many feasible configuration trajectory plans may exist that satisfy the terminal constraints,

*Draper Laboratory Fellow, Guidance and Navigation Division. Ph.D. Candidate, Dept. of Aeronautics and Astronautics, Massachusetts Institute of Technology.

†Senior Member of the Technical Staff, Guidance and Navigation Division, Draper Laboratory, 555 Technology Square, Mail Stop 70, Cambridge, MA 02139.

in this research we are interested in determining a minimum-fuel configuration trajectory and corresponding thrust profile for each spacecraft. Given the desire to determine an optimal trajectory, the configuration problem is posed as an *optimal control problem*. Moreover, in this particular case the optimal control problem is highly nonlinear and has no analytic solution and, thus, must be solved numerically.

Several papers have attempted to solve tetrahedral formation optimization problems similar to the one considered in this paper. Ref. 3 uses a two-step approach that begins with genetic algorithms and afterwards refines the problem using Lawden's primer vector theory. Ref. 4 also uses a two-step approach, but combines a direct SQP method with a genetic algorithm. Ref. 5 employs a three-step approach that uses simulated annealing as its initial step. In each of these previous works, the problem is separated into pieces where, in general, one piece optimizes the orbital transfer portion of the trajectory and the other piece optimizes the relative position constraints in a sequential but separate optimization procedure that uses the trajectory from the first piece. While dividing the problem into parts and optimizing each part separately makes the problem more tractable, it also reduces the solution search space. Contrariwise, in this work the entire problem is formulated as a *single unified* numerical optimization procedure.

Numerical methods for solving optimal control problems fall into two general categories: indirect methods and direct methods. An excellent survey of various numerical methods for solving optimal control problems can be found in Ref. 7. In an indirect method, the first-order optimality conditions are derived using the minimum principle of Pontryagin.[8] These necessary conditions lead to a Hamiltonian boundary-value problem (HBVP) which is then solved to determine candidate optimal trajectories called extremal trajectories. In a direct method, the optimal control problem is discretized at specified time points called nodes (common discretization methods used in direct methods include trapezoidal, Hermite-Simpson, and Runge-Kutta[9]). The discretized problem is then transcribed to a nonlinear programming problem (NLP) and the NLP is solved using an appropriate optimization method such as those described in Ref. 6 and Ref. 10.

In recent years, direct methods have risen to prominence.[11] The reason for the relatively widespread use of direct methods is that, as compared to indirect methods, direct methods are capable of solving a much wider range of complex problems. Furthermore, direct methods are superior to indirect methods because it is easier to find a solution to the NLP than it is to find a solution to the associated HBVP. Well-known software packages employing direct methods include *Optimal Trajectories by Implicit Simulation* (OTIS),[12] *Sparse Optimal Control Software* (SOCS),[13] *Graphical Environment for Simulation and Optimization* (GESOP),[14] *Direct Collocation* (DIRCOL),[15] and *Direct and Indirect Dynamic Optimization* (DIDO).[16]

A recently developed class of methods that have shown promise in the numerical solution of optimal control problems are *pseudospectral methods*.[17–20] In a pseudospectral method, the state and control are parameterized using a basis of globally orthogonal polynomials.[17] Two particular pseudospectral methods that have been previously developed are the *Legendre pseudospectral method*[18,19] and the *Chebyshev pseudospectral method*.[20] It is noted that the Legendre pseudospectral method has been applied to a wide variety of applications including atmospheric entry,[21] orbital transfer,[22] and trajectory design for a two spacecraft formation.[23]

In this research we are interested in applying a newly developed pseudospectral method, called the *Gauss Pseudospectral Method*,[24] to the problem of minimum-fuel spacecraft formation configuration. In the Gauss pseudospectral method, the state and control are approximated using a basis of globally orthogonal Lagrange polynomials. The problem is then discretized at a set of points called *Gauss points* (it is noted that the discretization points for the Gauss pseudospectral method differ from discretization points in the Legendre pseudospectral method in that the Legendre pseudospectral method uses *Gauss-Lobatto* points). The

Gauss pseudospectral discretization leads to a discrete NLP that can be solved using a variety of well-known optimization algorithms (e.g. SNOPT[10] or SPRNLP[6]). Details of the Gauss pseudospectral method are found in Ref. 24.

In this paper, accurate numerical solutions are presented to the problem of minimum-fuel spacecraft configuration from an initial circular parking orbit of altitude 600 km to a terminal reference orbit of size 600 km by 7000 km. Furthermore, all numerical solutions in this research are obtained using the newly developed Gauss pseudospectral method of Ref. 24. More specifically, in this paper we study two configuration problems. In the first problem, the spacecraft are transferred from the initial parking orbit to the apogee of the reference orbit while simultaneously placing the formation in an acceptable tetrahedron. The second problem is an extension of the first problem in that the four spacecraft are required to achieve a repeating orbit by attaining the same positions at the second reference apogee that were attained at the first reference apogee. For the purposes of this study it is assumed that the spacecraft are point masses. Furthermore, the dynamics are modeled using modified equinoctial elements and the propulsion is modeled using finite thrust maneuvers. The optimal trajectories obtained in this study are highly consistent with physical intuition and provide insight into the structure of the optimally controlled system. Finally, the results obtained in this research demonstrate the general applicability of the Gauss pseudospectral method to the problem of spacecraft formation flying trajectory optimization.

2 SPACECRAFT FORMATION CONFIGURATION PROBLEM

Consider the problem of configuring a fleet of four spacecraft via orbital transfer from an initial parking orbit to a terminal reference orbit where the formation attains a desired tetrahedral shape at a specified point in the terminal reference orbit. Assuming that the four spacecraft are deployed simultaneously from the same launch vehicle or upper stage, each spacecraft starts at the same point on a circular orbit of altitude $h_0 = 600$ km and inclination $i_0 = 28$ deg. The desired terminal reference orbit is of size 600 km by 7000 km altitude with an inclination of 28 deg. In addition, at apogee of the terminal reference orbit the formation must be within 10 percent of a regular tetrahedron whose side-length is 10 km.

3 TRAJECTORY EVENT SEQUENCE

In this paper, we consider the following two trajectory configuration problems . The first problem, called the basic problem, terminates upon meeting the required tetrahedral position constraints the first time that the apogee of the reference orbit is attained. The second problem, called the extended problem, extends the first problem by one full orbit such that the terminal conditions attained upon reaching the second apogee are the same as those attained upon reaching the first apogee.

3.1 Trajectory Event Sequence for Basic Configuration Problem

The trajectory event sequence for the basic problem is given as follows. First, the trajectory is divided into four phases with the following sequence: coast, burn, coast, and burn. During the coast phases, it is assumed that the thrust is zero while during the burn phases it is assumed that the thrust is constant at its maximum value $T_{\max}$. Furthermore, at each phase interface it is assumed that the equinoctial elements and the mass are continuous, but that the control is discontinuous. Finally, the initial and terminal times of each phases are free (with the exception, of course, of the first phase where the initial time is fixed to zero). Fig. 1 shows a schematic of the basic configuration problem.

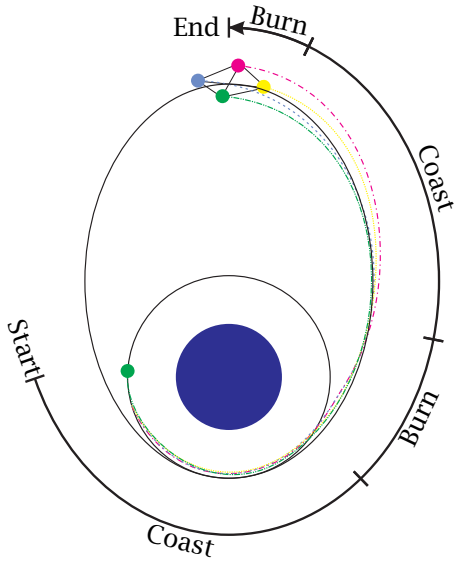

Figure 1: Schematic of Basic Configuration Problem.

3.2 Trajectory Event Sequence for Extended Configuration Problem

The trajectory event sequence for the extended problem is given as follows. First, the trajectory is divided into nine phases with the following sequence. The first four phases are the same at those of the basic problem while the remaining five phases have the following sequence: coast, burn, coast, burn, and coast. Furthermore, all of the assumptions during both the coast and burn phases are the same as those from the basic problem. Finally, all continuity conditions at the phase interfaces are the same as those from the basic problem. Fig. 2 shows a schematic of the basic configuration problem.

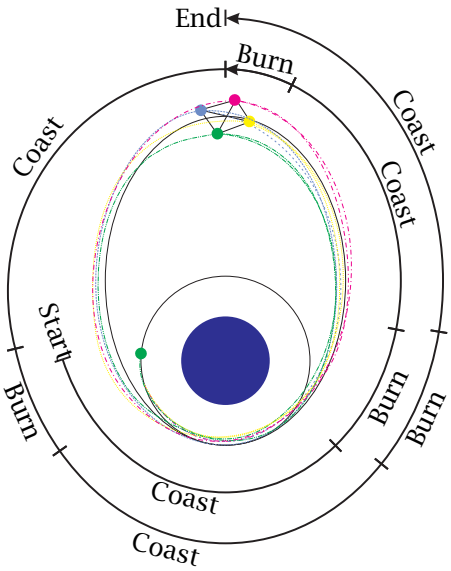

Figure 2: Schematic of Extended Configuration Problem.

4 EQUATIONS OF MOTION AND SPACECRAFT MODEL

4.1 Equations of Motion

The three degree-of-freedom equations of motion for a spacecraft moving over a spherical nonrotating Earth are given in modified equinoctial elements as[27]

$$\begin{aligned}
\dot{p} &= \frac{2p}{w}\sqrt{\frac{p}{\mu}}a_\theta \\
\dot{P}_1 &= \sqrt{\frac{p}{\mu}}\left\{-a_r\cos L + [(w+1)\sin L + P_1]\,\frac{a_\theta}{w} + [Q_2\sin L - Q_1\cos L]\,\frac{P_2 a_z}{w}\right\} \\
\dot{P}_2 &= \sqrt{\frac{p}{\mu}}\left\{a_r\sin L + [(w+1)\cos L + P_2]\,\frac{a_\theta}{w} - [Q_2\sin(L) - Q_1\cos L]\,\frac{P_1 a_z}{w}\right\} \\
\dot{Q}_1 &= \sqrt{\frac{p}{\mu}}\left(\frac{s^2}{2w}\right)a_z\sin L \\
\dot{Q}_2 &= \sqrt{\frac{p}{\mu}}\left(\frac{s^2}{2w}\right)a_z\cos L \\
\dot{L} &= \sqrt{\mu p}\left(\frac{w}{p}\right)^2 + \sqrt{\frac{p}{\mu}}\frac{Q_2\sin L - Q_1\cos L}{w}a_z
\end{aligned} \tag{1}$$

where p is the semi-latus rectum, L is true longitude, $w = p/r = 1 + P_1\sin L + P_2\cos L$, $s^2 = 1 + Q_1^2 + Q_2^2$, and a_r, a_θ, and a_z are the perturbing accelerations in the directions of $\mathbf{e}_r$, $\mathbf{e}_\theta$, and $\mathbf{e}_z$ where $\mathbf{e}_r$ is the unit vector in the radial direction, $\mathbf{e}_z$ is the unit vector in the direction normal to the orbital plane, and $\mathbf{e}_\theta = \mathbf{e}_z \times \mathbf{e}_r$ (thereby completing the right-handed system $\{\mathbf{e}_r, \mathbf{e}_\theta, \mathbf{e}_z\}$). For the application under consideration here, the perturbing accelerations are due entirely to thrust and can be written as

$$\begin{aligned}
a_r &= \frac{T}{m}u_r \\
a_\theta &= \frac{T}{m}u_\theta \\
a_z &= \frac{T}{m}u_z
\end{aligned} \tag{2}$$

where T is the thrust magnitude, m is the spacecraft mass, and u_r, u_θ, and u_z are the $\mathbf{e}_r$, $\mathbf{e}_\theta$, and $\mathbf{e}_z$ components, respectively, of the thrust direction. Finally, the mass flow rate of the engine is governed by the equation

$$\dot{m} = -\frac{T}{g_0 I_{sp}} \tag{3}$$

where g_0 is the sea level acceleration due to gravity and I_{sp} is the specific impulse of the engine.

4.2 Spacecraft Model

In this application we consider four identical spacecraft each with a dry mass of 200 kg and a fuel mass of 300 kg. Furthermore, the maximum thrust level of the engine is 7.015 kN with an engine specific impulse of 287.5 s. It is noted that these physical parameters are typical of a standard apogee kick motor.[28] Finally, all thrusting maneuvers are assumed to be non-impulsive.

5 CONSTRAINTS

5.1 Initial Conditions

All four spacecraft start in the same circular orbit at time $t = 0$. The initial conditions corresponding to this orbit are given in orbital elements as

$$\begin{array}{rclcrcl} a(0) & = & R_e + h_0 & , & e(0) & = & 0 \\ i(0) & = & 28 \text{ deg} & , & \omega(0) & = & 270 \text{ deg} \\ \Omega(0) & = & 0 & , & \nu(0) & = & 270 \text{ deg} \end{array} \tag{4}$$

where a is the semi-major axis, e is the eccentricity, i is the inclination, ω is the argument of perigee, Ω is the longitude of the ascending node, ν is the true anomaly, R_e is the radius of the Earth, and $h_0 = 600$ km is the initial altitude. It is noted that the initial argument of perigee, $\omega(0)$, is chosen to be the same as that of the terminal reference orbit while the initial true anomaly, $\nu(0)$, is arbitrary. The orbital elements in Eq. (4) are then converted to modified equinoctial elements using a transformation T_{o2e} (see for example Ref. 27) to obtain the initial state in modified equinoctial elements as

$$\begin{array}{rcl} p^{(i)}(t_0) & = & p_0 \\ P_1^{(i)}(t_0) & = & P_{1,0} \\ P_2^{(i)}(t_0) & = & P_{2,0} \\ Q_1^{(i)}(t_0) & = & Q_{1,0} \\ Q_2^{(i)}(t_0) & = & Q_{2,0} \\ L^{(i)}(t_0) & = & L_0 \end{array} \quad , (i = 1, \ldots, 4) \tag{5}$$

where i is the i^{th} spacecraft. Furthermore, the initial mass of each spacecraft is equal to its maximum value, i.e.

$$m^{(i)}(t_0) = m_{\max} \quad , \quad (i = 1, \ldots, 4) \tag{6}$$

where for this problem $m_{\max} = 500$ kg.

5.2 Interior Point Constraints

As stated earlier, in order for the trajectory to be continuous at each phase interface, it is necessary to enforce linkage conditions at every phase boundary. These linkage conditions are enforced on the modified equinoctial elements, mass, and time and are given as follows:

$$\begin{array}{rcl} p^{(i)}\left(t_f^{(j)}\right) & = & p^{(i)}\left((t_0^{(j+1)}\right) \\ P_1^{(i)}(t_f^{(j)}) & = & P_1^{(i)}\left(t_0^{(j+1)}\right) \\ P_2^{(i)}(t_f^{(j)}) & = & P_2^{(i)}\left(t_0^{(j+1)}\right) \\ Q_1^{(i)}(t_f^{(j)}) & = & Q_1^{(i)}\left(t_0^{(j+1)}\right) \\ Q_2^{(i)}(t_f^{(j)}) & = & Q_2^{(i)}\left(t_0^{(j+1)}\right) \\ L^{(i)}(t_f^{(j)}) & = & L^{(i)}\left(t_0^{(j+1)}\right) \\ m^{(i)}(t_f^{(j)}) & = & m^{(i)}\left(t_0^{(j+1)}\right) \\ \left(t_f^{(j)}\right)^{(i)} & = & \left(t_0^{(j+1)}\right)^{(i)} \end{array} \quad , \quad \begin{array}{c} (i = 1, \ldots, 4) \\ (j = 1, \ldots, P-1) \end{array} \tag{7}$$

where j is the j^{th} phase and P is the number of phases in the problem under consideration (in this case $P = 4$ for the basic problem and $P = 9$ for the extended problem). Finally, in order to ensure that time is increasing during the trajectory, the following inequality constraints are placed on the time during each phase of the trajectory:

$$\left(t_f^{(j)}\right)^{(i)} - \left(t_0^{(j)}\right)^{(i)} \geq 0 \quad , \quad (i = 1, \ldots, 4) \, , \, (j = 1, \ldots, P) \tag{8}$$

5.3 Path Constraints

During flight, the following two path constraints are imposed on the four spacecraft. First, during the thrust phases of the trajectory it is necessary to constrain the thrust direction to be unit length. Defining the thrust direction as $\mathbf{u}_T = \begin{bmatrix} u_r & u_\theta & u_z \end{bmatrix}^T$, the following constraint is imposed on $\mathbf{u}_T$ during the thrust phases:

$$\mathbf{u}_T \cdot \mathbf{u}_T = 1 \tag{9}$$

Second, during flight the mass of each spacecraft cannot fall below the vehicle dry mass. Defining the dry mass of each vehicle as m_{dry}, the following inequality constraint is imposed on the mass of each spacecraft during the each phase of the trajectory:

$$m^{(i)} \geq m_{\text{dry}} \quad , \quad (i = 1, \ldots, 4) \tag{10}$$

5.4 Terminal Constraints for Basic Problem

The position of the *mesocenter* of the formation is defined as

$$\bar{\mathbf{r}} = \sum_{i=1}^{4} \mathbf{r}^{(i)} \tag{11}$$

where $\mathbf{r}^{(i)}$, $(i = 1, \ldots, 4)$ are the positions of the four spacecraft as measured from the center of the Earth. The first constraint imposed on the formation at $t = t_f$ is that the mesocenter be located at the apogee of the reference orbit. Defining the position of the apogee of the reference orbit as $\mathbf{r}_a$, the constraint imposed on the position of the mesocenter of the formation at $t = t_f$ is given as

$$\bar{\mathbf{r}}(t_f) = \mathbf{r}_a \tag{12}$$

Next, let r_{rel} be the distance between a vertex of the desired regular tetrahedron and its mesocenter with a side length l. Then the square of the relative distance between each spacecraft and the mesocenter of the formation is constrained to be within 10 percent of r_{rel}^2 at $t = t_f$, i.e.

$$0.9 r_{\text{rel}}^2 \quad \leq \quad (\mathbf{r}^{(i)}(t_f) - \mathbf{r}_a) \cdot (\mathbf{r}^{(i)} - \mathbf{r}_a) \quad \leq \quad 1.1 r_{rel}^2 \quad , \quad (i = 1, \ldots, 4) \tag{13}$$

Third, the volume of the tetrahedron is constrained to be within 10 percent of the ideal volume of the desired regular tetrahedron at $t = t_f$, i.e.

$$0.9 V_I \quad \leq \quad V(t_f) \quad \leq \quad 1.1 V_I \tag{14}$$

where V_I is the volume of the ideal desired regular tetrahedron and V is the volume of the formation where the volume of a tetrahedron is given as

$$\begin{aligned} V &= \frac{8}{3}\sqrt{|\mathbf{R}|} \\ \mathbf{R} &= \frac{1}{4}\sum_{i=1}^{4} (\mathbf{r}^{(i)} - \bar{\mathbf{r}}) \otimes (\mathbf{r}^{(i)} - \bar{\mathbf{r}}) \end{aligned} \tag{15}$$

$|\mathbf{R}|$ is the determinant of the volumetric tensor, $\mathbf{R}$, and $\otimes$ is the tensor product between vectors. It is noted that the volume of a regular tetrahedron with side length l is given as

$$V_I = \frac{l^3\sqrt{2}}{12} \tag{16}$$

Finally, it is required that the trajectories of all four spacecraft terminate at the same time, i.e.

$$\left(t_f^{(P)}\right)^{(1)} = \ldots = \left(t_f^{(P)}\right)^{(4)} \tag{17}$$

where t_f is *free*.

5.5 Terminal Constraints for Extended Problem

In addition to the terminal constraints for the basic problem, the terminal constraints for the extended problem include a set of equality constraints that force the first five modified equinoctial elements at the end of phase 4 to equal the first five modified equinoctial elements at the end of phase 9. These equality constraints are given as

$$\begin{array}{rcl} p^{(i)}\left(t_f^{(4)}\right) & = & p^{(i)}\left((t_f^{(9)}\right) \\ P_1^{(i)}\left(t_f^{(4)}\right) & = & P_1^{(i)}\left(t_f^{(9)}\right) \\ P_2^{(i)}\left(t_f^{(4)}\right) & = & P_2^{(i)}\left(t_f^{(9)}\right) \\ Q_1^{(i)}\left(t_f^{(4)}\right) & = & Q_1^{(i)}\left(t_f^{(9)}\right) \\ Q_2^{(i)}\left(t_f^{(4)}\right) & = & Q_2^{(i)}\left(t_f^{(9)}\right) \end{array} \quad , \quad (i = 1, \ldots, 4) \tag{18}$$

In addition, in order for the spacecraft to return to the same location one full revolution after achieving the first apogee of the transfer orbit, it is necessary for the true longitude of each spacecraft at the end of phase 9 to be 2π greater than the true longitude of each spacecraft at the end of phase 4, i.e.

$$L^{(i)}\left(t_f^{(4)}\right) + 2\pi = L^{(i)}\left(t_f^{(9)}\right) \quad , \quad (i = 1, \ldots, 4) \tag{19}$$

Finally, the terminal times of each spacecraft in phase 4 must be equal to one another, i.e.

$$\left(t_f^{(4)}\right)^{(1)} = \ldots = \left(t_f^{(4)}\right)^{(4)} \tag{20}$$

6 OPTIMAL CONTROL SPACECRAFT CONFIGURATION PROBLEM

The optimal control spacecraft configuration problem is now stated formally. Using the aforementioned trajectory event sequence, determine the thrust profile that maximizes the sum of the terminal masses of each spacecraft, i.e. maximize the objective functional

$$J = \sum_{i=1}^{4} m^{(i)}(t_f) \tag{21}$$

subject to the differential equation constraints of Eq. (1) and Eq. (3), the initial constraints of Eq. (5) and Eq. (6), the interior point constraints of Eq. (7) and Eq. (8), the path constraints of Eq. (9) and Eq. (10), and the terminal constraints of *either* Eq. (12), Eq. (13) Eq. (14), and Eq. (17) for the basic problem *or* the terminal constraints of Eq. (12), Eq. (13) Eq. (14), Eq. (17), Eq. (18), Eq. (19), and Eq. (20) for the extended problem.

7 GAUSS PSEUDOSPECTRAL METHOD

The aforementioned optimal control problem can be written in the following general form. Minimize the cost functional

$$J = \Phi(\mathbf{x}(t_f), t_f) + \int_{t_0}^{t_f} g(\mathbf{x}(\tau), \mathbf{u}(t), t)dt \tag{22}$$

subject to the dynamic constraints

$$\frac{d\mathbf{x}}{dt} = \mathbf{f}(\mathbf{x}(t), \mathbf{u}(t), t) \tag{23}$$

and the boundary conditions

$$\boldsymbol{\phi}(\mathbf{x}(t_0), t_0, \mathbf{x}(t_f), t_f) = \mathbf{0} \tag{24}$$

In this research, the optimal control problem of Eq. (22)-Eq. (24) is solved using a newly developed direct transcription method called the *Gauss pseudospectral method*.[24] While it is beyond the scope of this paper to provide a detailed explanation of the Gauss pseudospectral method, a brief description is given here. The reader is referred to Ref. 24 for further details of the method.

The Gauss pseudospectral method (GPM) for a one-phase optimal control problem is summarized as follows. First, the original time interval $t \in [t_0, t_f]$, is transformed to the time interval $\tau \in [-1, 1]$ as

$$t = \frac{(t_f - t_0)\tau + (t_f + t_0)}{2} \tag{25}$$

Using the transformation of Eq. (25), the cost functional of Eq. (22) is then given in terms of τ as

$$J = \Phi(\mathbf{x}(1), t_f) + \frac{(t_f - t_0)}{2} \int_{-1}^{1} g(\mathbf{x}(\tau), \mathbf{u}(\tau), \tau) d\tau, \tag{26}$$

Similarly, the dynamic constraints of Eq. (23) are given in terms of τ as

$$\frac{2}{t_f - t_0} \frac{d\mathbf{x}}{d\tau} = \mathbf{f}(\mathbf{x}(\tau), \mathbf{u}(\tau), \tau), \tag{27}$$

Finally, the boundary conditions of Eq. (24) are given in terms of τ as

$$\boldsymbol{\phi}(\mathbf{x}(-1), t_0, \mathbf{x}(1), t_f) = \mathbf{0}. \tag{28}$$

Suppose now that we approximate the state, $\mathbf{x}(t)$ in terms of a basis of $N + 1$ Lagrange interpolating polynomials on the interval from $[-1, 1]$ as

$$\mathbf{x}(t) \approx \mathbf{X}(t) = \sum_{k=0}^{N} \mathbf{X}(t_k) L_k(t) \tag{29}$$

Furthermore, suppose we choose the following $N + 1$ points on $\tau \in [-1, 1]$ at which to discretize the continuous-time problem: the initial point $\tau = -1$ and N Gauss points, τ_k, $k = 1, \cdots, N$, which all lie on the interior of the interval $[-1, 1]$. The approximation to the derivative of the state at the Gauss points is then obtained as[24]

$$\left[\frac{d\mathbf{x}}{dt}\right]_{t_i} \approx \left[\frac{d\mathbf{X}^N}{dt}\right]_{t_i} = \sum_{k=0}^{N} \mathbf{X}_k \left(\frac{dL_k}{dt}\right)_{t_i} = \sum_{k=0}^{N} D_{ik} \mathbf{X}_k = \mathbf{f}(\mathbf{X}_i, \mathbf{U}_i, t_i) \tag{30}$$

where D_{ik} is called the *Differentiation Matrix*. It is noted that the differential operators $D \in \mathbb{R}^{N \times N}$ and $\bar{D} \in \mathbb{R}^N$ are found using the exact derivative of the Lagrange interpolating polynomials, $L_k(t)$ as

$$\left[\frac{d\mathbf{x}}{dt}\right]_{t_i} = \dot{\mathbf{x}}(t_i) \approx \dot{\mathbf{X}}(t_i) = \mathbf{X}(t_0) \cdot \bar{D}_i + \sum_{k=1}^{N} \mathbf{X}(t_k) \cdot D_{ik} \tag{31}$$

where $D_{ik} = \dot{L}_k(t_i)$ and $\bar{D}_i = \dot{L}_0(t_i)$ are the differential operators.

The continuous-time optimal control problem is discretized into a nonlinear programming problem (NLP) using the variables $\mathbf{X}_k \in \mathbb{R}^n$ for the states at the Gauss points and $\mathbf{U}_k \in \mathbb{R}^m$ for the control at the Gauss points, $k = 1, \cdots, N$. The initial and terminal states, $\mathbf{X}(t_0) \in \mathbb{R}^n$ and $\mathbf{X}(t_f) \in \mathbb{R}^n$, respectively, are also included as variables. First, the continuous-time cost functional of Eq. (26) is approximated using a Gauss quadrature as

$$J = \Phi(\mathbf{X}(t_f), t_f) + \frac{t_f - t_0}{2} \sum_{k=1}^{N} w_k g(\mathbf{X}_k, \mathbf{U}_k, t_k) \tag{32}$$

Where w_k are the Gauss weights. Next, the differential equation constraints of Eq. (27) are discretized at the Gauss points as

$$\frac{2}{t_f - t_0}\bar{D}_i\mathbf{X}(t_0) + \frac{2}{t_f - t_0}\sum_{k=1}^{N} D_{ik}\mathbf{X}_k = \mathbf{f}(\mathbf{X}_i, \mathbf{U}_i, t_i), \qquad i = 1, \cdots, N \tag{33}$$

where

$$[\ \bar{D}_i \quad D_{ik}\ ] = [\ (dL_0/d\tau)_{\tau_i} \quad (dL_k/d\tau)_{\tau_i}\ ] \in \mathbb{R}^{(N+1)\times(N+1)} \tag{34}$$

It is noted that, unlike previously developed pseudospectral methods,[18,20] the differential equations are collocated only at the Gauss points and not at the boundary points. Then, the discretized boundary conditions are given as

$$\boldsymbol{\phi}(\mathbf{X}(t_0), t_0, \mathbf{X}(t_f), t_f) = \mathbf{0} \tag{35}$$

Finally, the terminal state, $\mathbf{X}(t_f)$, is defined using a quadrature approximation to the dynamics as

$$\mathbf{X}(t_f) = \mathbf{X}(t_0) + \frac{t_f - t_0}{2}\sum_{k=1}^{N} w_k\mathbf{f}(\mathbf{X}_k, \mathbf{U}_k, t_k) \tag{36}$$

The cost function of Eq. (32) and the constraints of Eq. (33) and Eq. (35) define an NLP. The solution of this NLP is an approximate solution to the continuous-time optimal control problem.

It is noted that the Gauss pseudospectral method has been extended to problems with multiple phases (see Ref. 24). The extension to a P-phase problem involves repeating the structure for the one-phase formulation P times. Furthermore, the terminal constraints for the first phase, the initial and terminal constraints for the interior phases, and the initial constraints for the P^{th} phase are replaced by interior point constraints. The phases are then linked together using continuity conditions similar to those seen in Eq. (7) and Eq. (8). In addition to the ability to handle multiple phases, the Gauss pseudospectral method is readily extendible to problems involving multiple vehicles by concatenating the state and control of each spacecraft, thereby forming a single higher dimensional state and control. The optimal control problem can then be posed in the form given above.

8 NUMERICAL SOLUTION VIA GAUSS PSEUDOSPECTRAL METHOD

The spacecraft configuration problem as described in section 2 - section 6 is solved using the aforementioned Gauss pseudospectral method of Ref. 24. The optimization was carried out with the MATLAB mex interface of the NLP solver SNOPT[29] using analytic first-order derivatives for the constraint Jacobian and the gradient of the objective function. Furthermore, in all cases the optimal control problem was scaled from SI units to an alternate set of units using a length scale of the radius of the Earth and a time scale of one Schuler period. All other quantities were scaled to maintain a canonical transformation. Furthermore, it is important to note that the values of tetrahedral volume in this scaled set of units are extremely small as compared to the norm of the gradient of the volume. Consequently, in order to properly scale the volume and its derivatives, the terminal constraint of Eq. (14) was implemented in the basic problem by taking the 20^{th} root of the volume, i.e. in the basic problem Eq. (14) was implemented as

$$[0.9V_I]^{1/20} \quad \leq \quad \left[V(t_f)\right]^{1/20} \quad \leq \quad [1.1V_I]^{1/20} \tag{37}$$

Similarly, the terminal constraint of Eq. (14) was implemented in the extended problem by taking the 25^{th} root of the volume, i.e. in the extended problem Eq. (14) was implemented as

$$[0.9V_I]^{1/25} \quad \leq \quad \left[V(t_f)\right]^{1/25} \quad \leq \quad [1.1V_I]^{1/25} \tag{38}$$

Finally, for both the basic and extended configuration problem, the optimization was carried out using 15 nodes (i.e. 13 Gauss points) for the thrust phases and 60 nodes (i.e. 58 Gauss points) for the coast phases.

9 RESULTS

The key results obtained in solving the aforementioned spacecraft configuration optimal control problem using the Gauss pseudospectral method are now summarized. The first subsection summarizes the results for the basic problem while the second subsection summarizes the results for the extended problem. For both sets of results it is noted that the initial orbit of each spacecraft is 600 km circular while the terminal reference orbit is 600 km by 7000 km.

9.1 Results for Basic Problem

The key features of the optimal solution for the basic problem are summarized in Figs. 3-6. Fig. 3 provides a three-dimensional perspective of the terminal tetrahedron for the basic problem where $x - \bar{x}$, $y - \bar{y}$ and $z - \bar{z}$ are the components of the position of each spacecraft relative to the mesocenter where x, y, and z are the measured in a standard Earth-centered inertial coordinate system.[26] It is interesting to observe from Table 1 that, despite the presence of two burn opportunities, each spacecraft thrusts only during the first burn phase, i.e. the optimal duration of the second burn phase is zero. Furthermore, as seen in Fig. 5, the optimal locations of the nonzero thrust maneuvers for each of the spacecraft are near the terminal reference perigee, consistent with intuition. Upon closer inspection of Fig. 5, it is seen that all four burns are offset by varying amounts from the terminal reference perigee. It is this staggering of the burns that allows the spacecraft to meet the terminal position and timing constraints without the need for multiple maneuvers. Also, from Fig. 4 and Fig. 5, it is seen that the amount of fuel burned by each spacecraft increases as the burns depart from the terminal reference perigee. Moreover, by comparing Fig. 4 and Fig. 6 it is seen that the amount of fuel burned by each spacecraft increases with increasing terminal altitude (again, consistent with intuition). It is noted that the terminal semi-major axis also increases with increasing terminal altitude and results in a different terminal semi-major axis for each spacecraft. Finally, as seen in Fig. 6, the component of position orthogonal to the orbital plane is nearly the same for all four spacecraft. In fact, using the law of cosines to determine the required impulsive ΔV to change inclination,[30] it can be shown that an increase in inclination requires a disproportionately large increase in ΔV. Consequently, the fuel-minimizing solution attempts to reduce the maximum out-of-plane component of all four spacecraft.

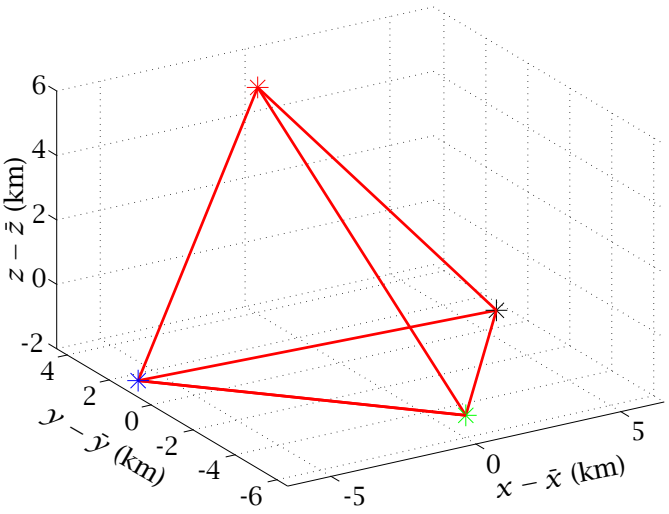

Figure 3: Three-Dimensional View of Optimal Terminal Tetrahedron for Basic Configuration Problem.

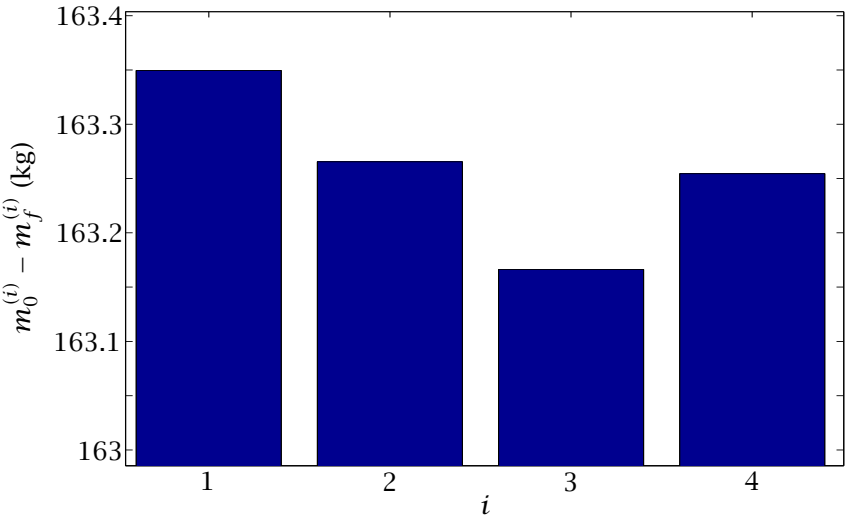

Figure 4: Optimal Fuel Consumption $m_0^{(i)} - m_f^{(i)}$ of Spacecraft $i = 1, \ldots, 4$ for Basic Configuration Problem.

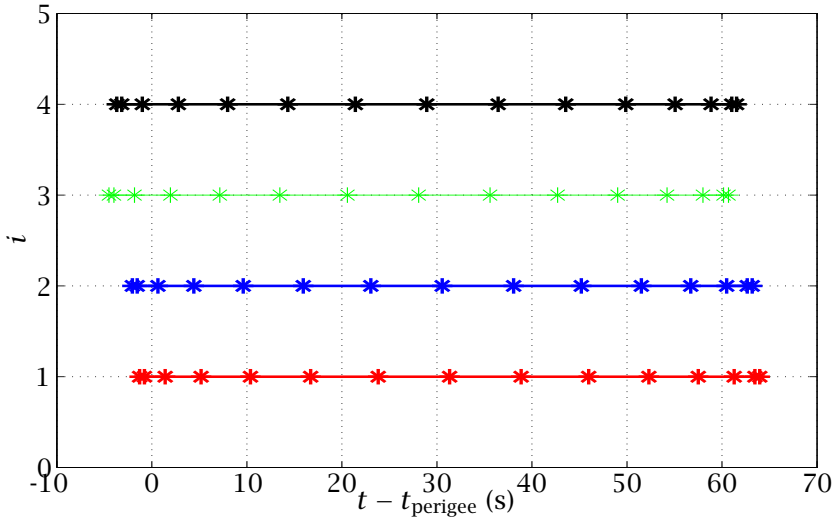

Figure 5: Spacecraft Burn Durations Relative to Time of Reference Perigee Passage, $t - t_{\text{perigee}}$, for Spacecraft $i = 1, \ldots, 4$ During First Burn Phase for Basic Configuration Problem.

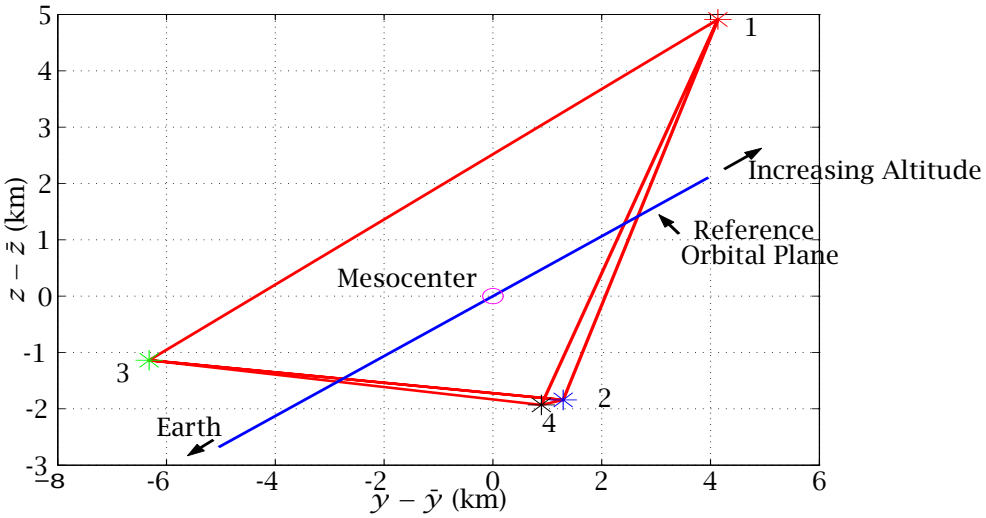

Figure 6: Optimal Terminal Tetrahedron Viewed Along Orbital Plane for Basic Configuration Problem.

Table 1: BURN TIMES FOR BASIC PROBLEM

Burn Duration (s) \ Spacecraft Number	1	2	3	4
First Burn	65.2634	65.2298	65.1901	65.2254
Second Burn	0	0	0	0

9.2 Results for Extended Problem

The key features of the extended problem are shown in Figs. 8-10. We note several key differences between the optimal trajectories of the basic problem and the extended problem. First, because of the terminal constraint on the true longitude as given in Eq. (18), it is required that each spacecraft return to the same position *exactly* one period after attaining the first apogee. We recall that the period of a spacecraft in orbit is given as[27]

$$P = 2\pi\sqrt{\frac{a^3}{\mu}} \tag{39}$$

From the relationship in Eq. (39), the fuel-optimal solution of the extended problem requires that all four spacecraft have the same semi-major axis at the first reference apogee. This requirement is unlike the basic problem where all four spacecraft can have different semi-major axes. The spacecraft then passively return to their exact positions one period later, thus eliminating the need for maneuvers during the second orbit as seen in Table 2. This implicit constraint on the semi-major axis results in two conflicting demands on the problem. On the one hand, the optimizer wants to set all semi-major axes equal. However, in order to form a tetrahedron, all four spacecraft must be placed at different terminal altitudes (and therefore different semi-major axes). In order to satisfy both of these demands simultaneously, at least one of the spacecraft must perform an additional maneuver. In particular, it is seen again from Table 2 that in the optimal solution to the extended problem, one of the four spacecraft performs a burn near apogee of the reference orbit. The fuel mass expended near the reference apogee for spacecraft 1 is seen in Fig. 8.

Second, Fig. 7 and Fig. 10 show a three-dimensional view and view along the orbital plane, respectively, of the optimal terminal tetrahedron for the extended problem. Consistent with the results of the basic problem, as seen in Fig. 8, the fuel burned near reference perigee increases with increasing terminal altitude. Moreover, the initial maneuvers near reference perigee in the extended problem result in spacecraft 2, 3, and 4 terminating with the same semi-major axis. Consequently, spacecraft 2, 3, and 4 have approximately the same terminal altitude as seen in Fig. 10. While spacecraft 2, 3, and 4 all have similar terminal altitudes, it is noted that spacecraft 3 and spacecraft 4 burn slightly more fuel than spacecraft 2 (as seen in Fig. 8) due to the fact that spacecraft 3 and 4 must maneuver out of the reference orbital plane. Spacecraft 1 (whose altitude is significantly different from the other three spacecraft) is required to perform an addition burn near the reference apogee in order to achieve the same semi-major axis as the other three spacecraft. Lastly, consistent with the results of the basic problem, the amount of fuel burned increases as the burns depart from the reference perigee. Interestingly, Fig. 9 shows that spacecraft 3 and spacecraft 4 begin their perigee burns *after* passing the reference perigee (unlike spacecraft 1 and 2 in the extended problem and all four spacecraft in the basic problem), although it is unclear what effect this has on the trajectory.

Third, unlike the basic problem (where all four spacecraft terminate moderately out of the reference orbital plane), Fig. 10 shows that, in the extended problem, two of the spacecraft terminate significantly out of the reference orbital plane. While this last result for the extended problem appears contrary to the results obtained in the basic problem (where the maximum out-of-plane position was much smaller), it is important to note that in the extended problem it is necessary that all four spacecraft terminate with the same semi-major axis. The results of the extended problem show that it is more fuel efficient to align semi-major axes than it is to reduce the maximum out-of-plane component of position of all four spacecraft. These results also suggest that the tetrahedron orientation in the basic problem may be infeasible in the extended problem.

The aforementioned results of the basic and extended problems leads to perhaps the most interesting result of this paper: that the tetrahedron, (whose orientation was left uncon-

strained in the problem formulation) actually has a fuel-optimal orientation. As seen in Fig. 10, the fuel-optimal orientation is approximately symmetric about the orbital plane, with the out-of-plane spacecraft (3 and 4) leading the in-plane spacecraft (1 and 2) along the trajectory. Further research is required to determine how this orientation changes with the addition of different perturbation effects.

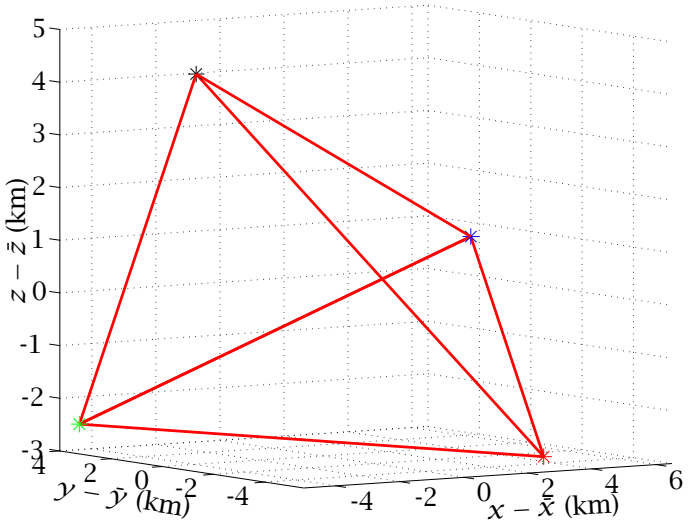

Figure 7: Three-Dimensional View of Optimal Terminal Tetrahedron for Extended Configuration Problem.

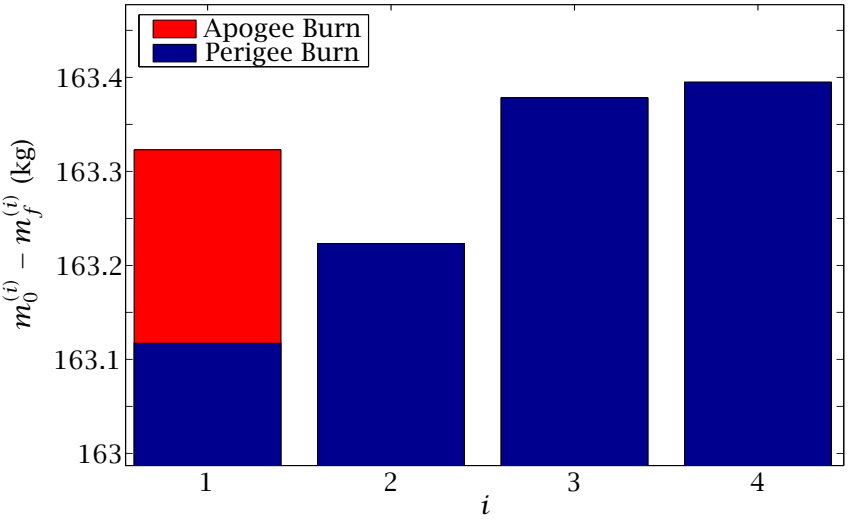

Figure 8: Optimal Fuel Consumption $m_0^{(i)} - m_f^{(i)}$ of Spacecraft $i = 1,\ldots,4$ for Extended Configuration Problem.

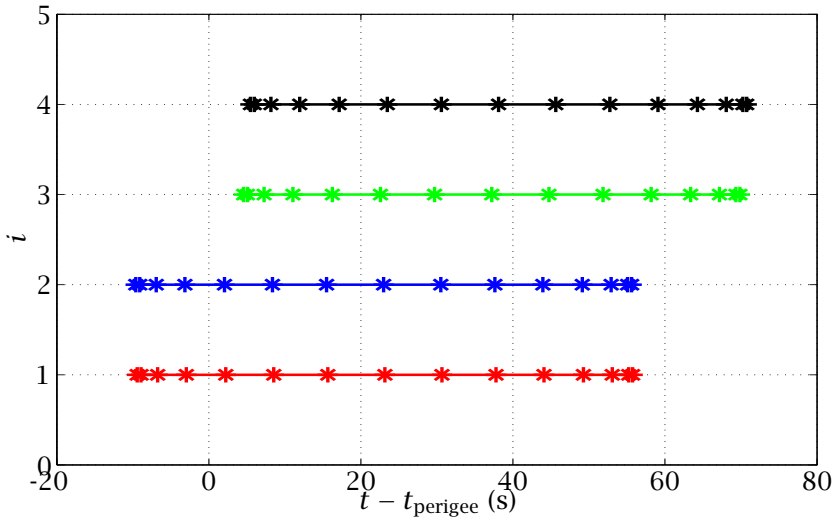

Figure 9: Spacecraft Burn Durations Relative to Time of Reference Perigee Passage, $t - t_{\text{perigee}}$, for Spacecraft $i = 1, \ldots, 4$ During First Burn Phase for Extended Configuration Problem.

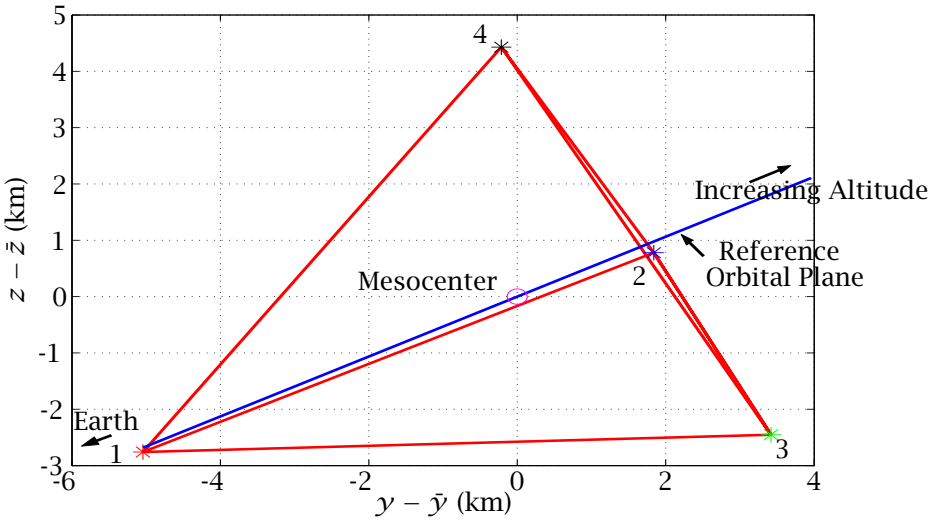

Figure 10: Optimal Terminal Tetrahedron Viewed Along Orbital Plane for Extended Configuration Problem.

Table 2: BURN TIMES FOR EXTENDED PROBLEM

Burn Duration (s) \ Spacecraft Number	1	2	3	4
First Burn	65.1705	65.2129	65.2749	65.2815
Second Burn	0.0822	0	0	0
Third Burn	0	0	0	0
Fourth Burn	0	0	0	0

10 CONCLUSIONS

The problem of determining minimum-fuel maneuver sequences for a four-spacecraft formation was considered. The objective was to determine fuel-optimal configuration trajectories that transfer a four spacecraft formation from an initial parking orbit to a desired terminal reference orbit while satisfying particular formation constraints. The configuration problem was solved numerically using a newly developed direct transcription method called the *Gauss pseudospectral method*. In particular, two versions of the minimum-fuel configuration problem were considered. In the first problem the trajectory was terminated upon satisfying the required terminal position constraints. In the second problem the trajectory was extended one full orbit beyond that of the first problem such that the terminal conditions are the same as those attained one period earlier. Finally, the key features of both optimal configuration problems were discussed. The results of this research provide insight into the structure of formation configuration trajectories and demonstrate the applicability of the Gauss pseudospectral method to optimal formation flying trajectory design.

DISCLAIMER

Any opinions, findings, and conclusions or recommendations expressed in this material are those of the authors and do not necessarily reflect the views of the National Aeronautics and Space Administration.

ACKNOWLEDGMENTS

This work was funded by the NASA Goddard Spaceflight Center under Cooperative Agreement NAS5-NCC5-730. The authors would like to thank Mr. Stephen P. Hughes as technical monitor for his insights and helpful suggestions during the course of this work. The authors would also like to thank Dr. David A. Benson for his help both with the understanding and the implementation of the Gauss pseudospectral method.

REFERENCES

1. Scharf, D. P., Hadaegh, F. Y., and Ploen, S. R., "A Survey of Spacecraft Formation Flying Guidance and Control (Part II): Control," *Proceedings of the American Control Conference*, Boston, MA, pp. 2976–2985, 2004.
2. Scharf, D. P., Hadaegh, F. Y., and Ploen, S. R., "A Survey of Spacecraft Formation Flying Guidance and Control (Part I): Guidance," *Proceedings of the American Control Conference*, Denver, CO, pp. 1733-1739, 2003.
3. Mailhe, Laurie M., Guzman, Jose J., "Initialization and Resizing of Formation Flying using Global and Local Optimization Methods," *Proceedings of the IEEE Aerospace Conference*, Big Sky, Montana, paper #1425, 2004.
4. Guzman, Jose J. "Tetrahedron Formation Control," *Journal of the Astronautical Sciences*, Vol. 51, No. 4, pp. 419-431, 2003.
5. Tsuda, Y., "Global Optimization of Maneuver Schedule for Multiple Spacecrafts Flying in Formation," *55th International Astronautical Congress*, Vancouver, Canada, IAC-04-A.2.01, 2004.
6. Betts, J. T. and Frank, P. D., "A Sparse Nonlinear Optimization Algorithm," *Journal of Optimization Theory and Applications*, Vol. 82, pp. 519-541, 1994.
7. Betts, J. T., "Survey of Numerical Methods for Trajectory Optimization," *Journal of Guidance, Control, and Dynamics*, Vol. 21, No. 2, 1998, pp. 193–207.
8. Athans, M. and Falb, P. L., *Optimal Control*, McGraw-Hill, New York, 1966, pp. 284-351.
9. Betts, J. T.,, *Practical Methods for Optimal Control Using Nonlinear Programming*, Society for Industrial and Applied Mathematics Press, 2001.
10. Gill, P. E., Murray, W., and Saunders, M. A., "SNOPT: An SQP Algorithm for Large-Scale Constrained Optimization," *SIAM Journal on Optimization*, Vol. 12, No. 4, 2002, pp. 979–1006.

11. Hargraves, C. R. and Paris, S. W., "Direct Trajectory Optimization Using Nonlinear Programming and Collocation," *Journal of Guidance, Control, and Dynamics*, Vol. 10, No. 4, 1987, pp. 338-342.
12. Vlases, W. G., Paris, S. W., Lajoie, R. M., Martens, M. J., and Hargraves, C. R., "Optimal Trajectories by Implicit Simulation," Boeing Aerospace and Electronics, Technical Report WRDC-TR-90-3056, Wright-Patterson Air Force Base, 1990.
13. Betts, J. T. and Huffman, W. P., "Sparse Optimal Control Software - SOCS," Mathematics and Engineering Analysis Library Report, MEA-LR-085, Boeing Information and Support Services, P. O. Box 3797, Seattle, WA, 98124-2297, 15 July 1997.
14. Well, K., *Graphical Environment for Simulation and Optimization*, Department of Optimization, Guidance, and Control, Stuttgart, Germany, 2002.
15. Von Stryk, O., "User's Guide for DIRCOL 2.1: A Direct Collocation Method for the Numerical Solution of Optimal Control Problems," Technische Universitat Darmstadt, 1999.
16. Ross, I. M. , "User's Manual for DIDO (Ver. PR.1β): A MATLAB Application Package for Solving Optimal Control Problems", *Technical Report 04-01.0*, February 2004.
17. Canuto, C., Hussaini, M.Y., Quarteroni, A., Zang, T.A., *Spectral Methods in Fluid Dynamics,* Springer-Verlag, New York, 1988.
18. Elnagar, G., Kazemi, M., Razzaghi, M., "The Pseudospectral Legendre Method for Discretizing Optimal Control Problems," *IEEE Transactions on Automatic Control*, Vol. 40, No. 10, October 1995.
19. Fahroo, F. and Ross, I. M., "Co-state Estimation by a Legendre Pseudospectral Method," *Journal of Guidance, Control, and Dynamics*, Vol. 24, No. 2, March-April 2002, pp. 270-277.
20. Fahroo, F. and Ross, I. M., "Direct Trajectory Optimization by a Chebyshev Pseudospectral Method," *Journal of Guidance, Control, and Dynamics*, Vol. 25, No. 1, January-February 2002, pp. 160–166.
21. Rao, A. V. and Clarke, K. A., "Performance Optimization of a Maneuvering Re-entry Vehicle Using a Legendre Pseudospectral Method," *2002 AIAA Atmospheric Flight Mechanics Conference*, AIAA Paper 2002-4885, Monterey, CA August 5–8, 2002.
22. Stanton, S. and Proulx, R., "Optimal Orbital Transfer Using a Legendre Pseudospectral Method," *AAS/AIAA Astrodynamics Specialist Conference*, AAS-03-574, Big Sky, Montana, August 3–7, 2003.
23. Ross, I., King, J., and Fahroo, F., "Designing Optimal Spacecraft Formations," *2002 AIAA/AAS Astrodynamics Specialist Conference*, AIAA Paper 2002-4635, Monterey, CA, August 5–8, 2002.
24. Benson, D., *A Gauss Pseudospectral Transcription for Optimal Control*, Ph.D. Dissertation, Department of Aeronautics and Astronautics, Massachusetts Institute of Technology, November 2004.
25. Holmstrom, K., Goran, A. O., and Edvall, M., "User's Guide for TOMLAB 4.5," TOMLAB Optimization, 23 November 2004.
26. Chobotov, V. A., Ed., *Orbital Mechanics*, AIAA Press, New York, 1991, p. 18.
27. Battin, R. H., *An Introduction to the Mathematics and Methods of Astrodynamics*, AIAA Press, New York, 1987, pp. 490-493 and p. 119.
28. Wertz, J. R. and Larsen, W. J., *Space Mission Analysis and Design*, 3^{rd} Edition, Microcosm Press, El Segundo, CA and Kluwer Academic Publishers, Dordrecht, The Netherlands, 1999, p. 694.
29. Gill, P.E., *Users Guide for SNOPT Version 7, A Fortran Package for Large-Scale Nonlinear Programming,* University of California, San Diego, La Jolla, CA, Sept 04.
30. Wiesel, William E., *Spaceflight Dynamics*, McGraw-Hill Companies, Inc., New York, 1997, pp. 75-76.